RESEARCH ARTICLE

Maternal Epidermal Growth Factor Promotes Neonatal Claudin-2 Dependent Increases in Small Intestinal Calcium Permeability

Megan R. Beggs [1,2], Kennedi Young[1], Allen Plain[1], Debbie D O'Neill[1],
Ahsan Raza[3], Veit Flockerzi[3], Henrik Dimke[4,5], R. Todd Alexander[1,2,6,*]

[1]Department of Physiology, University of Alberta, Edmonton, AB T6G 2H7, Canada, [2]The Women's & Children's Health Research Institute, Edmonton, AB T6G 1C9, Canada, [3]Experimentelle und Klinische Pharmakologie und Toxikologie, Saarland University, 66421 Homburg, Germany, [4]Department of Cardiovascular and Renal Research, Institute of Molecular Medicine, University of Southern Denmark, Odense C DK-5000, Demark, [5]Department of Nephrology, Odense University Hospital, 5000 Odense C, Denmark and [6]Department of Pediatrics, University of Alberta, Edmonton, AB T6G 1C9, Canada

*Address correspondence to R.T.A. (e-mail: todd2@ualberta.ca)

Abstract

A higher concentration of calcium in breast milk than blood favors paracellular calcium absorption enabling growth during postnatal development. We aimed to determine whether suckling animals have greater intestinal calcium permeability to maximize absorption and to identify the underlying molecular mechanism. We examined intestinal claudin expression at different ages in mice and in human intestinal epithelial (Caco-2) cells in response to hormones or human milk. We also measured intestinal calcium permeability in wildtype, *Cldn2* and *Cldn12* KO mice and Caco-2 cells in response to hormones or human milk. Bone mineralization in mice was assessed by μCT. Calcium permeability across the jejunum and ileum of mice were 2-fold greater at 2 wk than 2 mo postnatal age. At 2 wk, *Cldn2* and *Cldn12* expression were greater, but only *Cldn2* KO mice had decreased calcium permeability compared to wildtype. This translated to decreased bone volume, cross-sectional thickness, and tissue mineral density of femurs. Weaning from breast milk led to a 50% decrease in *Cldn2* expression in the jejunum and ileum. Epidermal growth factor (EGF) in breast milk specifically increased only CLDN2 expression and calcium permeability in Caco-2 cells. These data support intestinal permeability to calcium, conferred by claudin-2, being greater in suckling mice and being driven by EGF in breast milk. Loss of the CLDN2 pathway leads to suboptimal bone mineralization at 2 wk of life. Overall, EGF-mediated control of intestinal claudin-2 expression contributes to maximal intestinal calcium absorption in suckling animals.
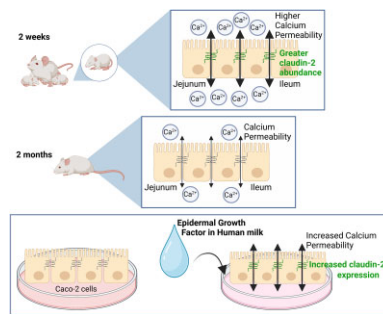
Key words: calcium; intestine; development; EGF; permeability; paracellular; mineral

Introduction

Periods of rapid growth, such as during postnatal development, require optimal intestinal absorption of calcium to meet demands of building bones. Intestinal absorption occurs via both transcellular and paracellular pathways. We previously described novel pathways contributing to transcellular Ca^{2+} absorption that occur only early in infancy.[1] However, given the high concentration of Ca^{2+} in breast milk relative to serum, intestinal absorption via paracellular diffusion also presents an energetically favorable pathway to provide a large amount of Ca^{2+} to enable growth.[2] It is not known if the paracellular pathway contributes to enhanced Ca^{2+} uptake in infancy nor whether it is regulated to facilitate greater Ca^{2+} absorption during postnatal development.[3]

The tight junction proteins claudin-2 (gene *CLDN2*) and claudin-12 (gene *CLDN12*), members of the claudin family, have been implicated in forming Ca^{2+} permeable pores across intestinal and renal epithelia[4,5] that facilitate paracellular Ca^{2+} absorption. Claudin proteins interact within and between epithelial cells to form selective barriers and pores and thus confer specific permeability properties across epithelial tissue. In the murine proximal colon, claudin-2 and claudin-12 form independent, Ca^{2+} permeable pores, which contribute calcium permeability (P_{Ca}) across the tissue.[6,7] Both *Cldn2* and *Cldn12* are also expressed in the renal proximal tubule with *Cldn12* KO mice displaying decreased P_{Ca} and *Cldn2* KO animals displaying hypercalciuria, consistent with a role in renal Ca^{2+} reabsorption.[8,9] In both mice and humans, intestinal *CLDN2* expression is higher early in life.[10–12] However, previous work has not examined whether this higher level of gene expression translates to higher claudin-2 or -12 protein levels, which may then confer greater P_{Ca} to the small intestine during postnatal development. Additionally, regulation of these pathways is not fully understood.

We therefore sought to determine if P_{Ca} across the small intestine changes with age and if claudin-2 or -12 regulation facilitates greater paracellular Ca^{2+} permeability at a young age. Based on the need for high Ca^{2+} deposition during development, we hypothesized that intestinal Ca^{2+} permeability would be greater early in life to optimize Ca^{2+} absorption for bone growth and that claudin-2 or -12 would confer this greater P_{Ca}. By examining the impacts of claudin-2 or -12 expression *in vivo* during early postnatal life, we found that P_{Ca} across the jejunum and ileum are 2-fold higher before weaning than after, and that this greater P_{Ca} is conferred by higher *Cldn2* expression and CLDN2 abundance. *Cldn2* deletion results in decreased bone mineralization early in life despite evidence of compensatory intestinal transcellular Ca^{2+} absorption and decreased Ca^{2+} excretion into urine. Moreover, we show that epidermal growth factor (EGF)

present in human breast milk increases CLDN2 expression and P_{Ca} across a human epithelial Caco-2 cell monolayer, uncovering a mechanism for this regulation. Thus overall, we propose that EGF-mediated increases in intestinal claudin-2 expression facilitates greater uptake of dietary Ca^{2+} in suckling animals.

Materials and Methods

Study Approval

Animal experiments were approved by the University of Alberta animal ethics committee, Health Sciences Section (AUP00000213). Written informed consent was provided by participants who donated breast milk samples as approved by the University of Alberta Health Research Ethics Board—Biomedical Panel (Pro00100603).

Animals

Wild-type FVB/N (Taconic labs, North America), global *Cldn2* KO (MMRRC at University of California, Davis), global *Cldn12* KO[9] and mice with a nonfunctioning pore mutation in TRPV6 (*Trpv6*^{mt})[13] were maintained on a 12-h light/dark cycle with drinking water and standard chow (Lab Diet Irradiated Rodent Diet 5053 4.5% fat) available ad libitum. Global KO mice and TRPV6 mutant mice had been backcrossed onto the FVB/N background for 9 generations. Early weaning experiments were described previously.[1] Litter mates were used to compare WT and KO animals.

Ca^{2+} Permeability Across Intestinal Segments and In-Vitro

Bi-ionic diffusion potential experiments were performed on intestinal segments and Caco-2 cells as described previously.[6,7,14] Fresh tissue was excised and mounted into Ussing chambers (VCC multichannel Voltage/Current Clamp, Physiologic Instruments, San Diego, CA). Tissue was bathed bilaterally with 4 mL Krebs buffer (140 mM Na^+, 5.2 mM K^+, 120 mM Cl^-, 1.2 mM Mg^{2+}, 1.2 mM Ca^{2+}, 2.8 mM PO_4^-, 25 mM $HCO3$, pH 7.4) at 37°C and bubbled with 5% CO_2 (balance O_2). Where indicated, nifedipine (Sigma-Aldrich; cat.# N7634) was added to a final concentration 10 μmol L^{-1} apically. The tissue was allowed to stabilize for 15 min and then three 90 μA current pulses were applied to calculate transepithelial resistance (TER) using Ohm's law. The clamp was then turned off and the tissue left in an open circuit setting enabling the potential difference (voltage) across the tissue to be monitored. The basolateral chamber was then filled with "control" Krebs-Ringer buffer (144 mM Na^+, 3.6 mM K^+, 146 mM Cl^-, 1 mM Mg^{2+}, 1.3 mM Ca^{2+}, 2 mM PO_4^-,

3 mм HEPES, pH 7.4) at 37°C and the apical buffer was changed to a low NaCl solution (30 mм Na$^+$, 3.6 mм K$^+$, 32 mм Cl$^-$, 1 mм Mg^{2+}, 1.3 mм Ca^{2+}, 2 mм PO$_4^-$, 3 mм HEPES, pH 7.4). The low NaCl solution was kept iso-osmotic to the control solution with the addition of mannitol. The resulting peak change in transepithelial voltage was used to determine the permeability ratio of Na$^+$ to Cl$^-$ (P$_{Na}$/P$_{Cl}$) Goldman–Hodgkin–Katz (GHK) voltage equation for monovalent positive and negative ion species where the activity of other ions apart from Na$^+$ and Cl$^-$ were negligible in the experimental conditions at this step of the protocol where a large sodium and chloride concentration gradient was imposed. A simplified Kimizuka–Koketsu equation was then used to calculate absolute permeability. The calculations employed for these determinations have also been previously described.[4,14–18] The apical buffer was then changed to the control buffer and TER was measured as above after the potential difference was stable. Due to the fact that the GHK voltage equation is for monovalent ions, an ion flux approach was used to determine divalent cation permeability (ie, P$_{Ca}$).[6,7,9,14,15] Solutions were exchanged on both the basolateral (140 mм Na$^+$, 3.6 mм K$^+$, 146 mм Cl$^-$, 1 mм Mg^{2+}, 1.3 mм Ca^{2+}, 3 mм HEPES, pH 7.4) and apical sides (3.6 mм K$^+$, 146 mм Cl$^-$, 1 mм Mg^{2+}, 70 mм Ca^{2+}, 3 mм HEPES, pH 7.4) and the potential difference measured, which was used to calculate the relative P$_{Ca}$/P$_{Na}$ and absolute P$_{Ca}$ using published equations.[14] As previously described, solutions for determining ion permeabilities were bicarbonate-free to avoid precipitation and were buffered with HEPES.[14] Both buffers were finally changed back to the control buffer to measure TER. Tissue viability was considered as a TER change less than 40%.[19] All potential difference measurements were corrected for liquid junction potentials as previously described.[4] All basolateral buffers contained 10 mм dextrose. Osmolarity of all buffers was balanced using mannitol to 291 ± 1 mOsm (Advanced Instruments Model 3D3 osmometer). Experiments performed with Caco-2 cells employed the same culture medium and were grown as described below in the "Cell Culture" section. Cells were grown on a transwell culture filter insert (Corning Costar, Cat#3407). When milk, EGF, or erlotinib was added, it was added to the apical side. For experiments with the addition of milk to media, 2% milk by volume was added unless stated otherwise.

Ca^{2+} Flux Studies

Ca^{2+} flux studies were performed as previously and are further described below.[1,19] Briefly, fresh tissue was mounted into Ussing chambers connected to a VCC multichannel voltage/current clamp (Physiologic Instruments, San Diego, CA). Tissue was bathed bilaterally with 4 mL Krebs buffer (140 mм Na$^+$, 5.2 mм K$^+$, 120 mм Cl$^-$, 1.2 mм Mg^{2+}, 1.2 mм Ca^{2+}, 2.8 mм PO$_4^-$, 25 mм HCO3, pH 7.4) at 37°C and bubbled with 5% CO$_2$ (balance O$_2$). Indomethacin (Sigma-Aldrich Cat#17378) 2 μм bilaterally and tetrodotoxin (Alomone Labs, Jerusalem, Israel; Cat#T-550) 0.1 μм only basolaterally were added to inhibit prostaglandin synthesis and neuronal activity respectively. The basolateral buffer contained 10 mм glucose and the apical side 10 mм mannitol to balance osmolarity. The tissue was allowed to stabilize for 15 min and then TER calculated using Ohm's law after three 2 mV pulses were applied. One hemichamber was then spiked with 5 mCi mL^{-1} ^{45}Ca^{2+} (PerkinElmer Health Sciences, Waltham, MA) and the voltage clamp set to 0 mV to ensure there was no net driving force for paracellular ion diffusion present. Samples were taken from both chambers at 15-min intervals for 60

min. TER was again calculated and data omitted if TER changed by more than 40%.[19] Sample radioactivity was measured (LS6500 Multi-Purpose Scintillation Counter, Beckman Coulter, Brea, CA) and J$_{Ca}$ calculated as the rate of appearance of ^{45}Ca^{2+} in cpm h^{-1} into the cold chamber divided by the specific activity of the hot chamber in cpm mol^{-1} and normalized to surface area of tissue exposed. Data for basolateral to apical unidirectional fluxes by age were taken from previously published net J$_{Ca}$$^{2+}$ data.[1]

Quantitative Real-Time PCR

Quantitative PCR with specific primers and probes was performed as previous and sequences are listed in Table S1.[1,20,21] Total RNA was isolated using the TRIzol method (Invitrogen, Carlsbad, CA) with DNAse treatment (ThermoScientific, Vilnius, Lithuania). Five microgram total RNA, quantified with a Nanodrop 2000 (Thermo Fisher Scientific, Waltham, MA) was reverse transcribed (SensiFAST cDNA Synthesis Kit, FroggaBio, CA). Real-time PCR was then performed in triplicate for each cDNA sample (TaqMan Universal Master Mix II, ThermoFischer Scientific) with specific primers and probes (Integrated DNA Technologies) on a QuantStudio 6 Pro Real Time PCR System (ThermoFisher Scientific). Pooled RNA was used to create a standard mix of cDNA that was serially diluted to generate a standard curve and samples were quantified using the standard curve method. A C$_q$ value of greater than 35 was considered not detectable.

Immunohistochemistry of Intestinal Tissue

Freshly excised tissue was fixed in 10% formalin (Sigma Aldrich, Cat#F8775) then rinsed in PBS with 0.02% sodium azide (Fisher Chemical, Cat#S227I25). The tissue was embedded in paraffin, sectioned and stained for EGFR or CLDN2 essentially as described previously.[20,22] Rehydrated tissue was microwave boiled in Tris-EGTA buffer (TEG, 10 mм Tris, 0.5 mм EGTA, pH 9.0) for antigen retrieval. Free aldehyde groups were blocked in 0.6% H$_2$O$_2$ and 50 mм NH4Cl in PBS. Sections were blocked in 5% skim milk (Millipore Sigma Aldrich, Cat#70165), probed with primary antibody in 0.1% Triton-X100 in PBS overnight at 4°C and then incubated with secondary antibodies. Sections were visualized with DAB + Substrate Chromogen System (K3467, DakoCytomation) and counterstained with hematoxylin.

MicroCT of Bones

Femora from P14 WT and *Cldn-2* KO mice were analyzed by microCT and IHC as described previously.[1] Femora from p14 wild-type and *Cldn-2* KO mice were scanned with the resolution of 6.5 μm using a high resolution micro-CT system (Bruker, SkyScan 1172). The bones were wrapped within wet tissue paper, placed in a plastic holder and mounted vertically in the scanner sample chamber for imaging. X-rays source voltage and current were 49 kV and 200 μA, respectively. Beam hardening was reduced using a 0.5 mm Al filter. The exposure time was 5 s and scanning angular rotation was set to 180° with an increment of 0.4 deg rotation step.[23] NRecon (1.6.10.6) was used to reconstruct the images while other software like DataViewer (1.5.1.2) and CT Analyser (1.16.4.1+) from Bruker, MicroCT were used for bone analysis. A total number of 50 cross-sections exactly in the middle of femoral shaft were analyzed to access the cortical bone parameters.

Immunohistochemical Analysis of Bones

Histology to determine trabecular parameter of femurs from P14 WT and *Cldn2* KO mice were performed as previously described.[1] Freshly excised femurs were fixed in 4% PFA, incubated overnight in 30% sucrose, and then embedded in tissue freezing medium (simulated colonic environment medium; CEM-001; Section-Lab Co Ltd, Hiroshima, Japan). Four 6-μm sections in an anterior–posterior orientation were made at 2 different regions (minimum 100 μm spacing) for each bone. Two sections were stained with a modified toluidine blue to visualize cartilage and determine growth plate thickness. The mean of either two per bone was taken as a single value. Two sections were stained with alizarin red to visualize calcified bone and calculate trabecular parameters.

Determination of Electrolytes and Hormones

Urine electrolytes were measured by ion chromatography (Dionex Aquion Ion Chromatography System, Thermo Fisher Scientific). Samples were diluted 1:50 in ddH$_2$O with eluent of 4.5 mM Na$_2$CO$_3$/1.5 mM NaHCO$_3$ in ddH$_2$O for anions and 20 mM Methanesulfonic acid in ddH$_2$O for cations. Results were interpolated from a standard curved generated by serial dilutions of Dionex 5 anion and 6 cation-I standards (Dionex, Thermo Fisher Scientific Inc., Mississauga, ON, Canada) using Chromeleon 7 Chromatography Data System software (Thermo Scientific). Urine creatinine was measured using the Parameter creatinine kit (R&D systems, Minneapolis, MN). Plasma PTH (Immutopics Mouse Intact PTH 1–84), 1,25(OH)$_2$-vitamin D (Immunodiagnostic Systems Limited, Boldon, UK), FGF23 (Kainos Laboratories, Inc.) and milk EGF (Quantikine Human EGF Immunoassay, R&D systems) were measured by ELISA.

Cell Culture

Cell culture and immunoblots were performed as described previously.[1] Caco-2 cells (ATCC, Rockville, MD) were grown in DMEM supplemented with 10% FBS and 5% penicillin streptomycin glutamine at 37°C in 5% CO$_2$ in 6-well plates (Fisher Scientific, Cat#FB012927). For immunoblotting experiments, cells were seeded onto 100 mm dishes. When cells reached confluence, hormone, human breast milk, and/or erlotinib was added to the media for 48 h. Of note, EGF was undetectable by ELISA (Quantikine Human EGF Immunoassay, R&D systems) in both DMEM and FBS. EGF (Life Technologies Inc., Cat#PHG0311) was added to a final concentration of 100 ng mL^{-1}, vitamin D as calcitriol (Sigma-Aldrich, Cat#17936) to 20 nM,[24] prolactin (Sigma-Aldrich, Cat#SRP9000) at 400 ng mL^{-1} and Erlotinib (Sigma-Aldrich, Cat#SML2156) at 0.1 μM. Human milk was obtained as a random sample donated by volunteer participants and stored at −80°C until used for experiments. Milk was then added to cell culture media as % volume as indicated.

Immunoblot

Cells were lysed in RIPA buffer (50 mmol L^{-1} Tris, 150 mmol L^{-1} NaCl, 1 mmol L^{-1} EDTA, 1% Triton-X, 1% sodium dodecyl sulfate, 1% NP-40, pH 7.4) with phenylmethylsulfonyl fluoride to 1:1000 concentration (Thermo Scientific, Rockford, IL; cat.# 36978) and protease inhibitor set III to 1:100 concentration (Calbiochem, San Diego, CA; cat.# 535140) for 1 h on ice and then centrifuged for 10 min at 14 000 centrifugal force at 4°C. The protein content

of the supernatant was quantified using the Pierce 660 nm Protein Assay Reagent (ThermoFisher Scientific). Fifty microgram protein was run on 10% SDS-PAGE, electrotransferred to PVDF and blocked over night in TBST with 5% skim milk. Blots were incubated overnight at 4°C with primary antibody and 1 h at room temperature with secondary antibody. Primary antibodies used were mouse anti-claudin-2 (Cat#32–5600, ThermoFisher Scientific), rabbit anti-claudin-4 (Cat#PA1-37471, ThermoFisher Scientific), rabbit anti-claudin-7 (Cat#34–9100, Invitrogen), rabbit anti-claudin-10 (sc-25710, Santa Cruz Biotechnologies), and mouse anti-β-actin (BA3R, Invitrogen). HRP conjugated secondary antibodies employed included anti-rabbit (#7074, Cell Signaling, MA) and anti-mouse (#7076, Cell Signaling, MA).

Statistics and Data Availability

Individual data points in each graph represent data from one animal or experimental repeat. Both male and female animals were used for each experiment, and the numbers are in Table S2. Exploratory analysis found no differences between sexes. Sample sizes were based on previous publications.[1,6,7,9,19,20] Data were analyzed unblinded using GraphPad Prism 9.1.0. The Shapiro–Wilk test was used to evaluate for normal distribution and F test to compare variances. Data were analyzed and presented as indicated in figure and table legends. A $P < .05$ was considered statistically significant. The data underlying this article are available in the article and its online supplementary material.

Results

Intestinal Calcium Permeability Is Greater Prior to Weaning

In our previous work as part of assessing net transcellular Ca^{2+} flux across all segments of the small intestine in mice at postnatal day 14 (P14) and 2 mo of age,[1] we measured unidirectional basolateral to apical Ca^{2+} flux, which only occurs via the paracellular route due to the absence of transcellular calcium secretion into the intestinal lumen. When we compared basolateral to apical ^{45}Ca^{2+} flux across the small intestine of mice at P14 and 2 mo, we observed higher flux across the duodenum and jejunum at P14, suggesting higher Ca^{2+} permeability (P$_{Ca}$) across these segments early in life (Figure S1). Although no difference was observed across the ileum, this experimental design was originally intended to examine the transcellular Ca^{2+} transport pathway and so was conducted under conditions without an electrochemical driving force for paracellular Ca^{2+} diffusion. Therefore, we conducted further experiments to assess P$_{Ca}$ across the small intestine of young and older mice.

To directly assess P$_{Ca}$ along the small intestine of P14 and 2-mo-old mice, we performed bi-ionic diffusion potential experiments. There was slight, but significantly greater P$_{Ca}$ measured across the duodenum in mice at P14 in comparison to at 2 mo (Figure 1A). Moreover, the P$_{Ca}$ across the jejunum and ileum of mice at P14 was doubled that of the older animals at 2 mo (Figure 1B-C). In the duodenum, permeability to Na$^+$ (P$_{Na}$) is lower while TER and permeability to Cl$^-$ (P$_{Cl}$) are not different at P14. In the jejunum, TER is lower, P$_{Cl}$ is greater and P$_{Na}$ not different at P14. Across the ileum, TER and P$_{Na}$ are not different while P$_{Cl}$ is greater at P14. Moreover, the relative Ca^{2+} to Na$^+$ permeability (P$_{Ca}$/P$_{Na}$) significantly decreases from P14 to 2 mo in all segments (Tables S3–S5). The small intestine of younger mice therefore has greater P$_{Ca}$ and thus a greater capacity for Ca^{2+} absorption given
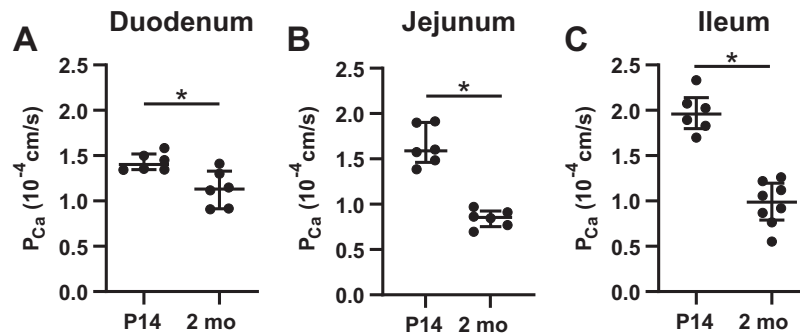
Figure 1. Calcium permeability across the small intestine is greater in young mice. (A) Duodenum ($P = .0152$), (B) jejunum ($P = .0022$), (C) ileum ($P = .0007$). Values presented as median and interquartile range. Analysis by Mann–Whitney test. P_{Ca}, Calcium permeability; P14, 2 wk old; 2 mo, 2 months old.

a 3–5-fold greater concentration of calcium in milk relative to blood.[25]

To exclude the possibility that the transcellular pathway might be contributing to the higher paracellular P_{Ca} measured in young animals, we performed further experiments. TRPV6 mediates transcellular Ca^{2+} uptake across the duodenum at 2 mo but not at P14.[1] To eliminate the possibility that TRPV6 was contributing Ca^{2+} permeability under our experimental conditions, P_{Ca} was measured across the duodenum of mice lacking functional Trpv6 (*Trpv6*[mt] mice) at 2 mo and found not to be different from WT mice of the same age (Figure S2A). Thus, the P_{Ca} observed is solely dependent on the paracellular pathway. Previous work also demonstrated that TRPV6 in the jejunum and $Ca_v1.3$ in the jejunum and ileum mediate net transcellular Ca^{2+} absorption at P14 but not 2 mo.[1] To exclude the possibility that these channels contribute to the greater P_{Ca} observed in younger mice in our experiments, we repeated the bi-ionic diffusion potential experiments on *Trvp6* WT and *Trpv6*[mt] mice and on WT mice in the presence or absence of the L-type Ca^{2+} channel blocker, nifedipine, at P14. No differences were observed in either tissue (Figure S2B–C). Together, these data strongly support the conclusion that paracellular P_{Ca} is higher across the small intestine of suckling mice than after weaning.

Cldn2 and *Cldn12* Expression Are Greater Along the Small Intestine Prior to Weaning

Previous *in vitro* and *ex vivo* work found that claudin-2 and claudin-12 contribute calcium permeability to intestinal epithelia.[5,6,9] We therefore hypothesized that the expression of one or both of these claudins is higher in younger mice and underlie the greater P_{Ca} observed. We examined claudin-2 and claudin-12 expression in the small intestine of mice from age P1 to 6 mo. We found that *Cldn2* expression was indeed higher in the jejunum and ileum of suckling pups at P1, P7, and P14, as compared to that of mice who are no longer suckling, that is, 1 mo of age and older. In the duodenum, *Cldn2* expression was greater at P1 and P7 but not at P14, relative to 1 mo (Figure 2A–C). To determine if CLDN2 protein is commensurately more abundant in younger animals, we stained fixed sections of intestine (Figure 2D–F) and observed strong junctional CLDN2 staining throughout the villi, where nutrient absorption occurs, and crypts along the small intestine at P14. By 2 mo of age, however, CLDN2 expression was less abundant in villi and strong staining found largely restricted to the crypts (Figure 2G–I), as reported previously for the jejunum.[11,12] *Cldn12* gene expression was

higher in the jejunum but not the duodenum or ileum of suckling mice (Figure 2J–L). Unfortunately, the lack of a specific antibody for claudin-12 precludes examining protein abundance.[9,26] These results suggest that either or both claudin-2 and claudin-12 confer the greater P_{Ca} observed in younger mice at P14 compared to at 2 mo.

Cldn2 Confers Greater Ca^{2+} Permeability Across the Jejunum and Ileum At P14

To assess the relative contributions of claudin-2 and claudin-12 to P_{Ca}, we repeated bi-ionic dilution potential studies in WT, *Cldn2* KO and *Cldn12* KO mice at P14 and 2 mo. P_{Ca} across the jejunum and ileum was significantly reduced in the P14 *Cldn2* KO mice. Moreover, P_{Ca} in the *Cldn2* KO P14 mice was no longer different from that at 2 mo, consistent with claudin-2 conferring the greater P_{Ca}. No difference was observed by genotype across any intestinal segment at 2 mo of age (Figure 3A–C). TER and permeability to Na^+ and Cl^- in the duodenum was not different by age or genotype. TER and PCl but not PNa decreased with age in the jejunum, while claudin-2 KO decreased TER and PNa at P14 but not 2 mo in the ileum (Tables S6–8). Unlike what we observed with *Cldn2* KO mice, bi-ionic diffusion potential experiments on tissue from WT and *Cldn12* KO mice revealed no differences between WT and *Cldn12* KO mice at any age or intestinal segment (Figure 3D–F). TER and permeability to Na^+ and Cl^- were not affected by genotype at either age (Tables S9–11). Taken together, these results are consistent with the greater P_{Ca} observed across the jejunum and ileum of younger mice being attributed to claudin-2.

Cldn2 KO Mice Display Impaired Bone Mineralization At P14

We hypothesized that the loss of *Cldn2*-mediated intestinal and renal permeability to Ca^{2+} would lead to an inability to maintain an optimal Ca^{2+} balance for bone mineralization during growth. We therefore examined the microarchitecture of femurs from *Cldn2* WT and KO mice at P14 (Table 1). We observed a significant decrease in cortical bone volume, cross-sectional thickness, and tissue mineral density in the *Cldn2* KO mice. No significant differences were observed in the parameters of trabecular bone. These results suggest that the greater P_{Ca} across the small intestine early in life conferred by claudin-2 is necessary to facilitate peak bone mineralization during this period of growth.
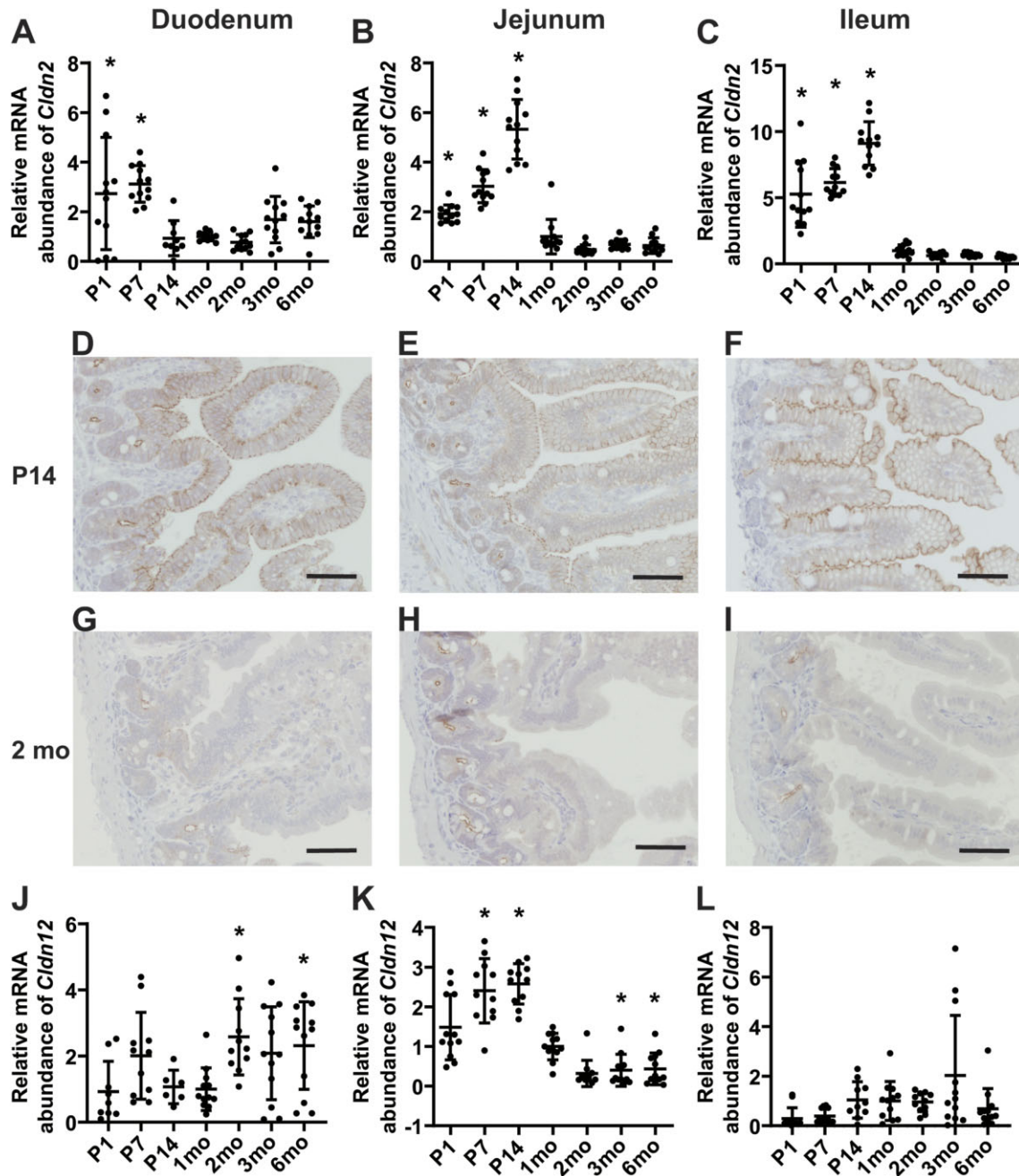
Figure 2. *Cldn2* and *Cldn12* expression varies with age along the small intestine. Relative expression of (A–C) *Cldn2* and (J–L) *Cldn12* from P1 to 6 mo of age in the duodenum (A and J), jejunum (B and K), and ileum (C and L). Expression is normalized to *Gapdh* and relative to 1 mo. Data presented as mean $\pm$ SD, *$P < .05$ vs 1 mo by ANOVA with Dunnett's multiple comparisons test. Immunoreactivity for CLDN2 was strong along both the villi and crypts of segments from (D) the duodenum, (E) the jejunum, and (F) the ileum at P14, whereas strong immunoreactivity was restricted to the crypts at 6 wk (G–I). Images were taken at 40$\times$ magnification and size bar indicates 50 μm. Representative images are obtained from evaluation of $n = 3$–4 mice per group.

P14 *Cldn2* KO Mice Exhibit Compensatory Reduction in Urinary Ca^{2+} Excretion and Higher Transcellular Ca^{2+} Flux Across the Jejunum

Given that claudin-2 mediates higher small intestine P_{Ca} at P14, we hypothesized that *Cldn2* KO mice at P14 would display intestinal and renal alterations to compensate for the loss of paracellular Ca^{2+} absorption. Indeed, we observed that urinary Ca^{2+} excretion normalized to creatinine was more than 2-fold lower in the *Cldn2* KO mice relative to WT (Figure 4A). This is partic-

ularly significant given that *Cldn2* KO mice at 8 weeks have a 3-fold increase in fractional Ca^{2+} excretion.[6,8] We next examined the expression of genes involved in renal Ca^{2+} reabsorption and found greater expression of *Trpv5*, *Calb1*, and *Atp2b1*, which together mediate transcellular Ca^{2+} reabsorption in the distal renal tubule (Figure S3). Thus, our results suggest compensatory increased renal Ca^{2+} reabsorption in the *Cldn2* KO pups that leads to decreased urinary Ca^{2+} excretion. Interestingly, we also observed decreased urinary phosphate, magnesium, and chloride excretion in the P14 *Cldn2* KO mice (Table S12).
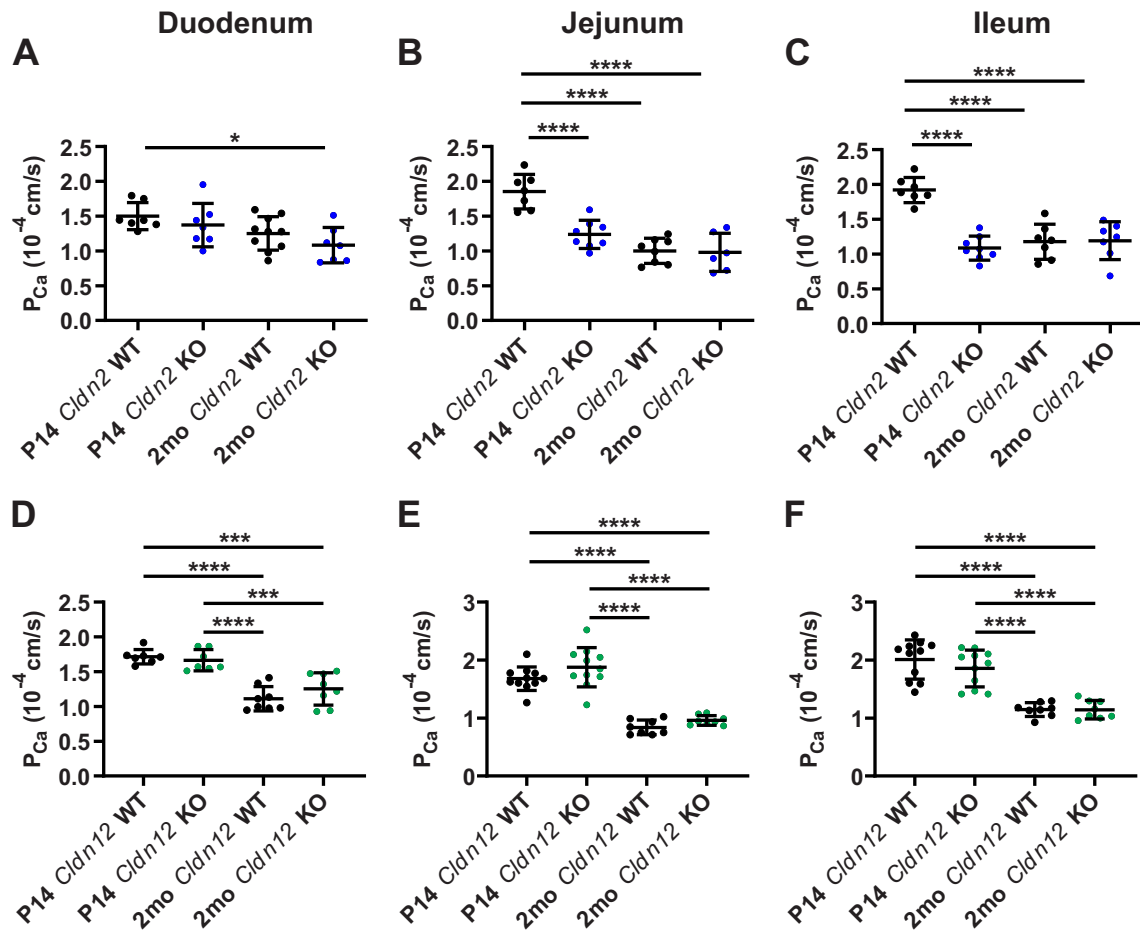
Figure 3. Claudin-2 confers greater P_{Ca} across jejunum and ileum in P14 mice. Calcium permeability across the duodenum (A, D), jejunum (B, E), and ileum (C, F) from *Cldn2* (A–C) and *Cldn12* (D–F) WT and KO mice at P14 and 2 mo. Data presented as mean $\pm$ SD and compared by one-way ANOVA with Tukey's multiple comparisons test, *$P < .05$, ***$P < .001$, ****$P < .0001$.

Table 1. Microarchitecture of femurs from *Cldn2* WT and KO mice at 2 wk

	WT	*Cldn2* KO	P-value
Cortical Bone			
N	7 (3 males)	6 (3 males)	
Tissue volume (mm^3)	0.322 $\pm$ 0.020	0.328 $\pm$ 0.016	.819
Bone volume (mm^3)	0.101 $\pm$ 0.005	0.085 $\pm$ 0.003	.034
Endocortical volume (mm^3)	0.221 $\pm$ 0.015	0.243 $\pm$ 0.013	.312
Cross-sectional thickness (mm)	0.081 $\pm$ 0.001	0.070 $\pm$ 0.001	< .001
Perimeter (mm)	3.72 $\pm$ 0.11	3.76 $\pm$ 0.10	.813
Femur length (mm)	9.07 $\pm$ 0.26	9.17 $\pm$ 0.19	.754
Tissue mineral density (g cm^{-3})	1.11 $\pm$ 0.01	1.07 $\pm$ 0.01	.023
Trabecular Bone			
N	6 (3 males)	6 (3 males)	
BV/TV (%)	24.6 $\pm$ 1.1	26.7 $\pm$ 1.3	.2487
Trabecular number (1 mm^{-1})	0.014 $\pm$ 0.0003	0.015 $\pm$ 0.0004	.0802
Trabecular width (μm)	17.9 $\pm$ 0.04	18.1 $\pm$ 0.6	.8686
Trabecular separation (μm)	55.5 $\pm$ 2.2	50.0 $\pm$ 2.4	.1175
Growth plate thickness (μm)	388. $\pm$ 18	396 $\pm$ 32	.8482

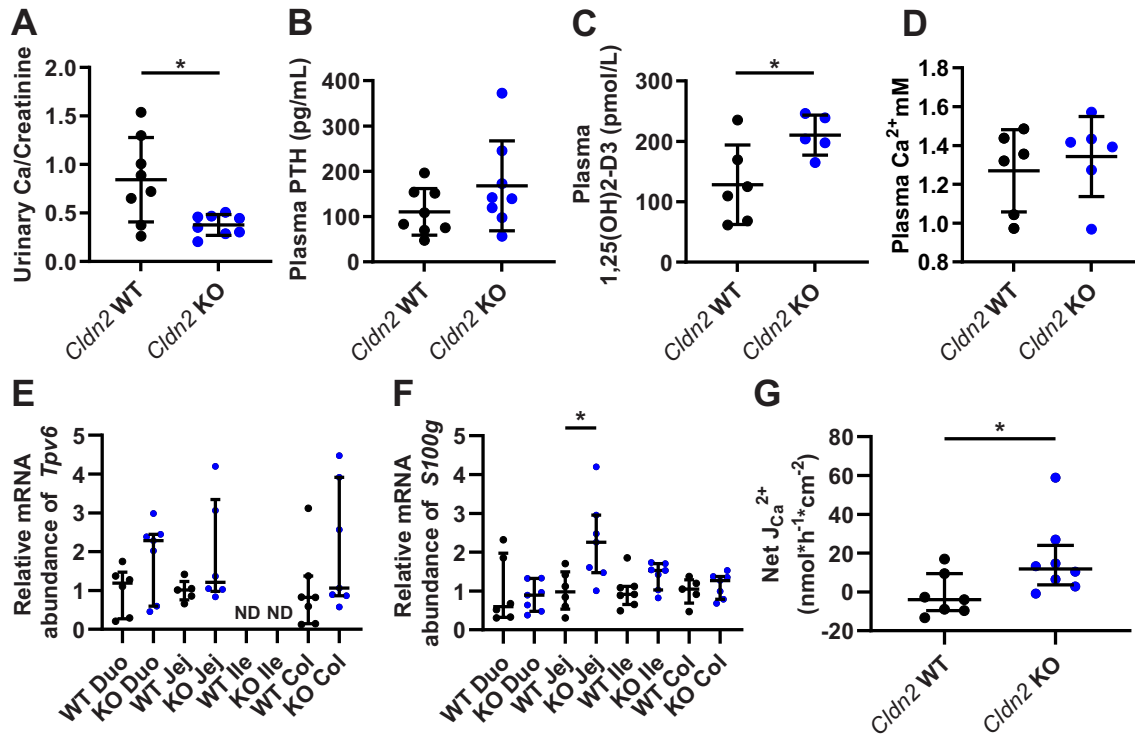BV/TV, bone volume/tissue volume. Data presented as mean $\pm$ SD and compared by unpaired *t*-test.

Figure 4. *Cldn2* KO pups at P14 display renal and intestinal compensation. (A) Urinary Ca^{2+} normalized to urinary creatinine ($P = .011$), (B) plasma PTH ($P = .1680$), (C) plasma calcitriol ($P = .0323$), and (D) plasma-ionized Ca^{2+} ($P = .8182$) in *Cldn2* WT and KO mice at P14. Data presented as mean $\pm$ SD and compared by unpaired *t*-test. Relative abundance of genes expressing (E) TRPV6 and (F) $Ca_v1.3$ in the intestine of WT and *Cldn2* KO mice at P14. Expression is normalized to β-*Actin* and presented relative to WT for each intestinal segment. (G) Net apical to basolateral $^{45}Ca^{2+}$ flux across *ex vivo* segments of jejunum from P14 mice ($P = .0289$). Each data point per segment represents an individual animal. Data presented as median $\pm$ IQR. Comparison of KO to WT for each intestinal segment by Mann–Whitney test. *$P < .05$. Duo, duodenum; Jej, jejunum; Ile, ileum; Col, colon. ND = not detected.

Serum Ca^{2+} is tightly regulated. Decreased plasma Ca^{2+} results in increased plasma active vitamin D (calcitriol) via parathyroid hormone (PTH) signaling to increase intestinal Ca^{2+} absorption and mobilization of Ca^{2+} from bone.[27,28] Plasma PTH was higher in the *Cldn2* KO mice, although not statistically different than WT (Figure 4B). However, plasma calcitriol was almost 1.6-fold greater in the *Cldn2* KO mice (Figure 4C). FGF-23 was not different between groups (Table S12). Overall, these compensatory mechanisms were adequate to maintain plasma-ionized Ca^{2+} (Figure 4D).

We next hypothesized that the increased plasma calcitriol would lead to increased expression of genes implicated in intestinal Ca^{2+} absorption of P14 *Cldn2* KO mice. The apical Ca^{2+} channels TRPV6 and $Ca_v1.3$ (which have been shown to mediate vectorial Ca^{2+} transport across the intestine) and the kinase TRPM7 have been suggested to be involved in intestinal transport of Ca^{2+}.[29] We therefore examined their expression in P14 WT and *Cldn2* KO mice intestines. The abundance of these three genes across all segments of the small intestine and proximal colon were not different (Figure 4E and Figure S4A–B). However, we found 2.3-fold greater expression of *S100g*, which encodes the intracellular binding protein calbindin-D_{9k} ($P = .0221$), in the jejunum of *Cldn2* KO mice (Figure 4F). No differences were observed in the expression of the basolateral Ca^{2+} extrusion proteins *Atp2b1* encoding PMCA1b, and *Slc8a1*, encoding NCX1 (Figure S4C–D). Increased *S100g* expression is consistent with greater influx of Ca^{2+} into the enterocyte.[30] Accordingly, we measured net apical to basolateral flux of $^{45}Ca^{2+}$ across *ex vivo* sections of the jejunum under conditions without an electrochemical gradient driving net paracellular diffusion. Indeed, the *Cldn2* KO mice at P14 had greater net apical to basolateral Ca^{2+} flux across this segment than WT littermates (Figure 4G). We also assessed for compensatory changes in other cation-pore forming claudins. We detected a 1.5-fold increase in both *Cldn12* and *Cldn15* in the duodenum (Figure S4E–F). Altogether, these results demonstrate renal and intestinal compensation for the loss of claudin-2 at P14 in mice.

Epidermal Growth Factor Is Present in Breast Milk and Increases *Cldn2* Expression

Given the correlation between increased Ca^{2+} uptake and *Cldn2* expression and the period pups are nursing, we next sought to determine if a bioactive compound is present in breast milk that mediates the higher P_{Ca} by increasing *Cldn2* expression. To test this hypothesis, half of a litter of pups was weaned early, at P12, to solid chow while the other half of the litter remained suckling with the dam for the following 48 h, then tissue was isolated and gene expression assessed. We found that *Cldn2* expression was lower by 50% in both the jejunum and ileum of mice that were no longer ingesting breast milk (Figure 5A–B). These results are consistent with breast milk containing a bioactive compound that acts to maintain or increase *Cldn2* expression. However, early weaning itself may also pose stress to the pups, which then leads to alterations in intestinal gene expression.[31,32] To specifically examine if breast milk regulates claudin-2 expression, we employed Caco-2 cells, an intestinal epithelial cell model, and incubated them with varying concentrations of breast milk from
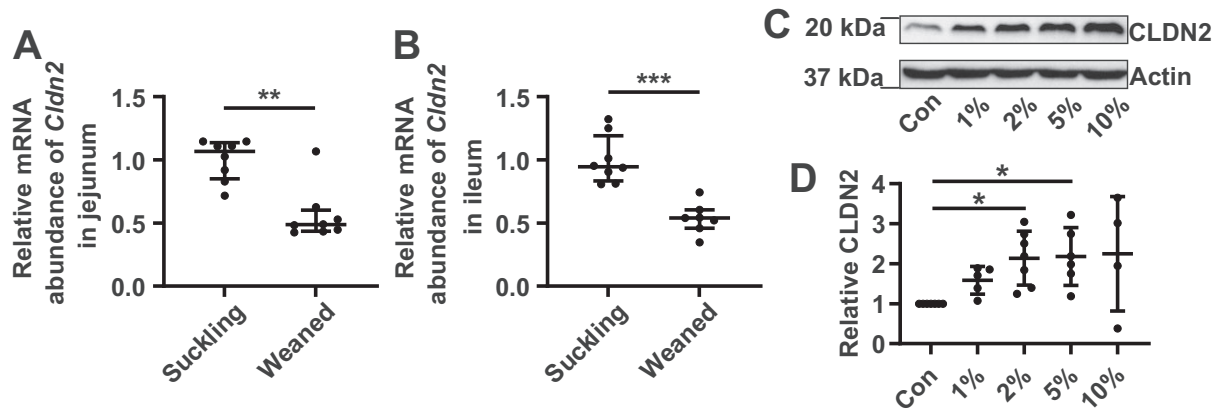
Figure 5. Breast milk increases intestinal expression of claudin-2. mRNA abundance of *Cldn2* in the (A) jejunum ($P = .0019$) and (B) ileum ($P = .0003$) of mice at P15 who remain with the dam (suckling) or who were weaned to solid chow at P12 (weaned). Expression is normalized to *β-Actin* and presented relative to suckling group as median ± IQR and compared by Mann–Whitney test. (C) Representative blots from 6 independent experiments of Caco-2 cells grown in media with increasing concentration as % by volume of human breast milk. (D) Semi-quantification of CLDN2 abundance from panel C normalized to *β*-actin and relative to control from the same blot. Data presented as mean ± SD and compared by one-way ANOVA with Tukey's multiple comparisons test. *$P < .05$, **$P < .01$, ***$P < .001$. Con, control.

human donors in the cell culture media. We observed increased CLDN2 expression when the concentration of milk in the cell culture media was 2%–5% (Figure 5C–D), consistent with a compound in breast milk mediating the effect. Expression of CLDN4, CLDN7, and CLDN10 (Figure S5A–D) were not altered by breast milk, consistent with a specific effect on CLDN2.

Candidates for a bioactive compound in breast milk include vitamin D, prolactin, and EGF. Vitamin D is known to increase claudin-2 expression, but its concentration in breast milk is very low, less than 1 nM and it is not present in the active form, calcitriol.[24,33] Prolactin is known to be present in breast milk and has also been proposed to increase Ca^{2+} absorption via both transcellular and paracellular pathways along the small and large intestine,[34–37] whereas EGF is present in murine and human breast milk and is known to alter claudin-2 expression, with different effects depending on the cell line.[31,38,39] To investigate the putative role of these signalling molecules in detail, we first confirmed the presence of EGF in our human breast milk samples. We found an average of 31.7 ± 23.1 ng mL^{-1} EGF, slightly lower than the published average of 83 ± 14 ng mL^{-1} but not unexpected as the mothers in the current study were further postpartum than in the previous published work.[40–42] We next confirmed that 20 nM calcitriol increased CLDN2 expression in this cell model as reported previously.[24] We found that 100 ng mL^{-1} EGF specifically increased CLDN2 expression, without affecting the expression of claudins 4, 7, or 10. Vitamin D increased and prolactin had no effect on CLDN2 expression in the Caco-2 intestinal epithelial cell model (Figure 6A–B and Figure S5E–H). These results suggest either vitamin D or EGF present in breast milk regulates intestinal CLDN2 expression.

To specifically implicate EGF in breast milk in regulating CLDN2 abundance, we cultured Caco-2 cells in the presence of the EGF receptor (EGFR) inhibitor erlotinib with or without media containing 2% breast milk (Figure 6C–D). Consistent with the previous experiments, the addition of breast milk increased CLDN2 abundance 2-fold. The addition of 0.1 μM erlotinib inhibited the milk-induced increase in CLDN2. These results specifically implicate EGF as the bioactive compound present in breast-milk that increases intestinal expression of *Cldn2* as erlotinib does not inhibit calcitriol activity.

We next performed bi-ionic diffusion potential experiments on Caco-2 cells grown under control conditions or with the addition of 100 ng mL^{-1} EGF to the media. P_{Ca} significantly increased 38% when cells were grown in the presence of EGF (Figure 6E). To test whether EGF in breast milk increases P_{Ca}, given it increases CLDN2 abundance, we repeated bionic diffusion potential experiments in Caco-2 cells grown with 2% breast milk in the media in the absence and presence of the EGFR inhibitor, erlotinib. Addition of erlotinib significantly decreased P_{Ca} when cells were grown with breast milk (Figure 6F). Consistent with results from murine tissue, P_{Na} was increased in the presence of EGF and decreased when erlotinib was added in addition to milk suggesting an effect on CLDN2 (Tables S13–14). Altogether, these results are consistent with EGF in breast milk increasing Ca^{2+} permeability across intestinal epithelia via increasing the abundance of claudin-2.

EGF exerts its actions via the plasma membrane EGFR. Therefore, if EGF present in breast milk is regulating intestinal expression of *Cldn2*, EGFR must be expressed in these intestinal cells. Indeed, *Egfr* is expressed in all segments of the small intestine and proximal colon of *Cldn2* WT and KO mice at P14, although no differences were found between genotypes (Figure S6A). Through immunohistochemical staining, we also found EGFR expression in the jejunum and ileum of mice at both P14 and 6 wk old (Figure S6B–E). We observed, however, more EGFR staining in 6-wk-old mice, likely due to upregulation as a consequence of reduced EGF exposure at this age when no longer nursing.

Discussion

We examined paracellular intestinal Ca^{2+} permeability during postnatal development to determine whether it is regulated to support greater Ca^{2+} absorption early in postnatal development. We found greater P_{Ca} across the jejunum and ileum of suckling mice compared to older mice. Using genetic knockout mouse models, we were able to attribute the greater intestinal P_{Ca} in young animals to higher claudin-2 expression. Loss of *Cldn2* resulted in decreased bone mineralization at 2 wk, despite compensatory increased transcellular intestinal Ca^{2+} absorption and renal reabsorption capacity. Furthermore, we implicate EGF in breast milk as the bioactive factor that increases CLDN2 abundance in a human intestinal epithelial cell model. Thus, we propose that a regulatory pathway through EGFR signaling
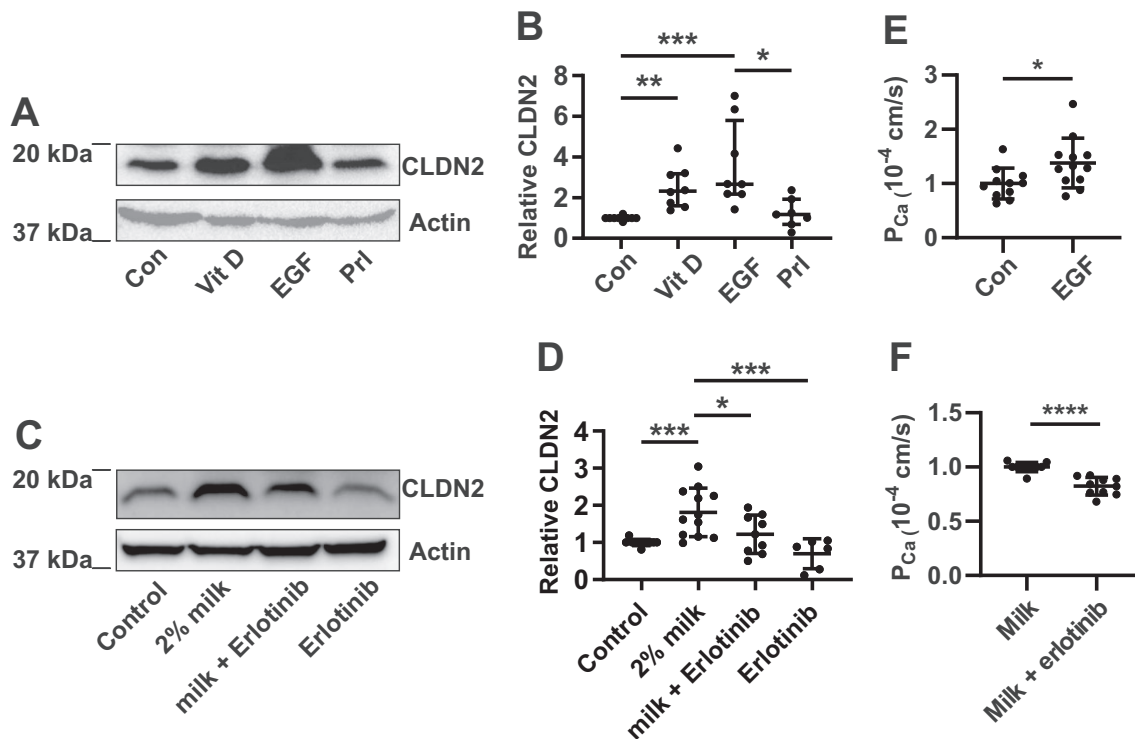
Figure 6. EGF in breast milk increases claudin-2 expression. (A) Representative blot from 7 independent experiments of Caco-2 cells grown in media with additional hormones as indicated. (B) Semi-quantification of CLDN2 abundance from panel (A) normalized to β-actin and relative to control from the same blot. (C) Representative blots from 3 to 6 independent experiments of Caco-2 cells grown with or without human breast milk and the EGFR inhibitor erlotinib (0.1 μM). (D) Semi-quantification of CLDN2 abundance from panel C normalized to β-actin and relative to control from the same blot. (E) Calcium permeability across Caco-2 monolayers grown without and with 100 ng mL^{-1} EGF normalized to control conditions. (F) Calcium permeability across Caco-2 monolayers in media containing 2% human milk without or with 0.1 μM erlotinib normalized to individual milk samples. $^*P < .05$, $^{**}P < .01$, $^{***}P < .001$, $^{****}P < .0001$. Con, control; VitD, calcitriol; EGF, epidermal growth factor; Prl, prolactin; milk, human milk; P_{Ca}, calcium permeability.

stimulated via breast milk that ensures greater intestinal paracellular Ca^{2+} absorption from the small intestine to meet the high demands required for optimal growth.

Physiologically, the paracellular pathway is energetically favorable as fewer proteins are required and, unlike the transcellular pathway, does not require ATP consumption.[2] In particular, diffusion down an electrochemical gradient is favorable under conditions of relatively high dietary Ca^{2+} intake such as occurs with a breast milk-only diet.[43] Dietary intake may explain why net absorption is observed across the small intestine of suckling rodents, whereas net secretion is observed across the jejunum and ileum of adult mice consuming normal chow because lower dietary Ca^{2+} intake alters the transepithelial driving force for paracellular Ca^{2+} absorption.[6,19,44–47]

Our findings are consistent with greater paracellular Ca^{2+} absorption from the small intestine resulting in net increased bone mineral accretion during the suckling period. A systematic review found that breastfeeding during infancy has a positive long-term impact on bone mass into adolescence, suggesting that infancy contributes to establishing lifelong bone health.[48] Between 3 and 11 wk of age in rats, intestinal Ca^{2+} absorption is equivalent to whole body Ca^{2+} retention and therefore, bone mineralization.[49] Similarly, in humans, Ca^{2+} retention and intestinal absorption are greatest during infancy and adolescence.[50] Previous studies in rats at 2, 3, and 6 wk of age and as adults suggests that the paracellular pathway predominates early in life and decreases with age but remains important for overall net absorption across the small intestine.[44,51] However,

we have previously shown that bone mineralization parameters are not different between *Cldn2* WT and KO animals at 10 wk of age.[6] Overall, this is consistent with the paracellular pathway being less significant after weaning and an ability for catch-up mineralization later, in the knockout animals at least.

In this study, we uncover new evidence supporting an important role of intestinal claudin-2 for overall Ca^{2+} balance early in life. Claudin-2 has previously been implicated in mediating Ca^{2+} permeability across intestinal and renal epithelia.[4–6] Consistent with our results, loss of *Cldn2* in mice decreased the cation permeability (P_{Na}) of the small intestine at 2 and 8 wk of age.[12] Our current and previous published work found greater claudin-2 expression in suckling animals.[11,12] In humans, children have a 3.3-fold greater claudin-2 abundance than adults in the duodenum,[10] leading to the suggestion that claudin-2 expression changes with age are independent of weaning. However, the pediatric population examined was 1–5 yr old, the age of weaning was not specifically stated, and other segments of the intestines were not examined.[10] Thus, it is possible that claudin-2 expression is even greater during infancy or that the jejunum and ileum have greater significance. Nonetheless, our results suggest that regulation of intestinal claudin-2 abundance presents a potential therapeutic target to maximize Ca^{2+} absorption for those with reduced bone mineralization.

EGF has long been recognized as a bioactive compound in breast milk and is also known to be present in saliva at all ages.[52–55] EGF in amniotic fluid and breast milk has a strong trophic effect on infant intestines and is associated with a

decreased risk of necrotizing enterocolitis (NEC) in premature infants.[56,57] In mice weaned early, EGF administration results in greater weight gain, villous height, crypt depth, and enterocyte proliferation.[31] EGF is critical for epithelial proliferation and repair throughout life and lower salivary levels are associated with small intestine ulcers.[57] Our study demonstrates that EGF specifically increases CLDN2 abundance in Caco-2 human intestinal epithelial cells. Similarly, previous studies revealed that addition of EGFR ligands (keratinocyte growth factor and amphiregulin) to growth media increases CLDN2 in this cell line.[58] Consistent with an effect of EGF in breast milk mediating greater claudin-2 expression, we found that weaning from breast milk leads to decreased *Cldn2* expression in infant mice. Moreover, the addition of the EGFR antagonist erlotinib to cells treated with breast milk prevented the increase in CLDN2 expression and decreased P_{Ca}. Therefore, in addition to previous investigations of EGF as a therapeutic for intestinal conditions, we present evidence for the potential of EGF as a therapeutic to modulate intestinal Ca^{2+} permeability enabling greater absorption and bone deposition during growth.

Our results are consistent with 20 nM calcitriol increasing the expression of claudin-2 in the Caco-2 cell model. However, the literature does not support a role for active vitamin D in breast milk altering claudin-2 expression. The vitamin D concentration in breast milk is very low, less than 1 nM and thus breast milk is likely not contributing biological activity.[59,60] In addition, the form of vitamin D in breast milk is largely as vitamin D and 25-hydroxyvitamin D, not the active form calcitriol that we demonstrate, and is known, to increase claudin-2 expression. While calcitriol is classically considered the active form of the hormone vitamin D that acts as a ligand for the vitamin D receptor (VDR), some studies have found that 25-hydroxyvitamin D may also be a low affinity ligand for VDR. Importantly, however, the concentration of this form of vitamin D required to alter downstream gene expression is many times greater than the concentration in breast milk, and is at least 100 nM or up to 500 nM depending on the cell type.[61–63] Therefore, we do not consider that vitamin D in breast milk is contributing to the effect of EGF on claudin-2 expression.

Although claudin-2 increases intestinal calcium permeability early in life, it also increases sodium permeability proportionately. Consequently P_{Ca}/P_{Na} was unaltered by the deletion of claudin-2 at either 2 wk of age or 2 mo. This calcium selectivity is not conferred by claudin-2, nor claudin-12. It is unknown what contributes selective calcium over sodium permeability to the intestine and is an area for future study. We did, however, observe greater absolute calcium permeability and relative calcium to sodium permeability (P_{Ca}/P_{Na}) at 2 wk, consistent with the need for greater calcium absorption at a young age.

A potential limitation of our current work is the lack of investigation of the large intestine. The colon is a major site of net Ca^{2+} absorption in adult humans and rodents, a process that may be mediated in some part by the microbiome.[19,64,65] Previous work by our group found that, at three months, *Cldn2* KO and *Cldn12* KO mice have decreased P_{Ca} across the proximal colon.[6,7] Further research is required to determine the contribution of the large intestine to net Ca^{2+} balance early in life. Our work is also limited by the use of Caco2 cells as a model system, which may not represent young intestinal epithelial. Future works should examine the effect of EGF on claudin-2 expression and intestinal P_{Ca} *in vivo*. Finally, we and others assess paracellular calcium permeability via the imposition of large gradients across the epithelia and the potential difference measured relatively quickly thereafter used to calculate relative and absolute ion permeabilities. Other methods, such as the use of radioactive tracers under voltage clamp or the imposition of smaller concentration gradients and measuring fluxes over longer periods of time may produce variations to these results. For this work, it is reassuring that our basolateral to apical flux experiments with calcium-45 revealed increased flux, consistent with our electrophysiological measurements.

In conclusion, we demonstrate that small intestine Ca^{2+} permeability is 2-fold greater in suckling vs adult mice. This greater capacity for paracellular Ca^{2+} absorption is conferred by greater claudin-2 expression induced by EGF in breast milk. Loss of this permeability results in suboptimal bone mineralization during this critical period of growth. This research elucidates a vital pathway to optimize intestinal Ca^{2+} absorption and highlights a potential therapeutic target.

Abbreviations

EGF—epidermal growth factor; EGFR—epidermal growth factor receptor; P_x—permeability to ion x; PTH—parathyroid hormone; TER—transepithelial resistance

Funding

Acknowledgments

Author Contributions

All authors contributed to experimental design, interpreting results, and manuscript revisions. M.R.B., K.Y., A.R., J.J.L., M.S., H.D. conducted experiments and analyzed data; H.D., P.W., V.F., and R.T.A. provided reagents and mice; M.R.B. wrote the first manuscript draft and all authors agreed on the final draft. A late draft was edited by Life Science Editors with funding from the the National Sciences and Engineering Research Souncil of Canada.

Supplementary Material

Supplementary material is available at the *APS Function* online

Conflict of Interest

None declared.

Data Availability

The data underlying this article are available in the article and in its online supplementary material.

References

1. Beggs MR, Lee JJ, Busch K, et al. TRPV6 and Cav1.3 mediate distal small intestine calcium absorption before weaning. *Cell Mol Gastroenterol Hepatol*. 2019;**8**(4):625–642.

2. Yu ASL. Paracellular transport as a strategy for energy conservation by multicellular organisms? *Tissue Barriers*. 2017;**5**(2):e1301852.

3. Beggs MR, Alexander RT. Intestinal absorption and renal reabsorption of calcium throughout postnatal development. *Exp Biol Med (Maywood)*. 2017;**242**(8):840–849.

4. Yu AS, Cheng MH, Angelow S, et al. Molecular basis for cation selectivity in claudin-2-based paracellular pores: identification of an electrostatic interaction site. *J Gen Physiol*. 2009;**133**(1):111–127.

5. Fujita H, Sugimoto K, Inatomi S, et al. Tight junction proteins claudin-2 and-12 are critical for vitamin D-dependent Ca^{2+} absorption between enterocytes. *MBoC*. 2008;**19**(5):1912–1921.

6. Curry JN, Saurette M, Askari M, et al. Claudin-2 deficiency associates with hypercalciuria in mice and human kidney stone disease. *J Clin Invest*. 2020;**130**(4):1948–1960.

7. Beggs MR, Young K, Pan W, et al. Claudin-2 and claudin-12 form independent, complementary pores required to maintain calcium homeostasis. *Proc Natl Acad Sci USA*. 2021;**118**(48).e2111247118. doi:10.1073/pnas.2111247118.

8. Muto S, Hata M, Taniguchi J, et al. Claudin-2 - deficient mice are defective in the leaky and cation-selective paracellular permeability properties of renal proximal tubules. *Proc Natl Acad Sci USA*. 2010;**107**(17):8011–8016.

9. Plain A, Pan W, O'Neill D, et al. Claudin-12 knockout mice demonstrate reduced proximal tubule calcium permeability. *IJMS*. 2020;**21**(6):2074.

10. Ong MLDM, Yeruva S, Sailer A, Nilsen SP, Turner JR. Differential regulation of claudin-2 and claudin-15 expression in children and adults with malabsorptive disease. *Lab Invest*. 2020;**100**(3):483–490.

11. Holmes JL, Van Itallie CM, Rasmussen JE, Anderson JM. Claudin profiling in the mouse during postnatal intestinal development and along the gastrointestinal tract reveals complex expression patterns. *Gene Expr Patterns*. 2006;**6**(6):581–588.

12. Tamura A, Hayashi H, Imasato M, et al. Loss of claudin-15, but not claudin-2, causes Na^+ deficiency and glucose malabsorption in mouse small intestine. *Gastroenterology*. 2011;**140**(3):913–923.

13. Weissgerber P, Kriebs U, Tsvilovskyy V, et al. Male fertility depends on Ca^{2+} absorption by TRPV6 in epididymal epithelia. *Sci. Signal*. 2011;**4**(171):ra27.

14. Günzel D, Stuiver M, Kausalya PJ, et al. Claudin-10 exists in six alternatively spliced isoforms that exhibit distinct localization and function. *J Cell Sci*. 2009;**122**(10):1507–1517.

15. Plain A, Wulfmeyer VC, Milatz S, et al. Corticomedullary difference in the effects of dietary Ca^{2+} on tight junction properties in thick ascending limbs of Henle's loop. *Pflugers Arch - Eur J Physiol*. 2016;**468**(2):293–303.

16. King AJ, Siegel M, He Y, et al. Inhibition of sodium/hydrogen exchanger 3 in the gastrointestinal tract by tenapanor reduces paracellular phosphate permeability. *Sci Transl Med*. 2018;**10**(456).eaam6474. https://doi.org/10.1126/scitranslmed.aam6474.

17. Kahle KT, Macgregor GG, Wilson FH, et al. Paracellular Cl-permeability is regulated by WNK4 kinase: insight into normal physiology and hypertension. *Proc Natl Acad Sci USA*. 2004;**101**(41):14877–14882.

18. Hou J, Paul DL, Goodenough DA. Paracellin-1 and the modulation of ion selectivity of tight junctions. *J Cell Sci*. 2005;**118**(21):5109–5118.

19. Rievaj J, Pan W, Cordat E, Alexander RT. The Na^+/H^+ exchanger isoform 3 is required for active paracellular and transcellular Ca^{2+} transport across murine cecum. *Am J Physiol-Gastrointest Liver Physiol*. 2013;**305**(4):G303–G313.

20. Beggs MR, Appel I, Svenningsen P, Skjødt K, Alexander RT, Dimke H. Expression of transcellular and paracellular calcium and magnesium transport proteins in renal and intestinal epithelia during lactation. *Am J Physiol Renal Physiol*. 2017;**313**(3):F629–F640.

21. Alexander RT, Beggs MR, Zamani R, Marcussen N, Frische S, Dimke H. Ultrastructural and immunohistochemical localization of plasma membrane Ca^{2+}-ATPase 4 in Ca^{2+}-transporting epithelia. *Am J Physiol Renal Physiol*. 2015;**309**(7):F604–F616.

22. van Megen WH, Tan RSG, Alexander RT, Dimke H. Differential parathyroid and kidney Ca^{2+}-sensing receptor activation in autosomal dominant hypocalcemia 1. *EBioMedicine* 2022;**78**:103947. doi:10.1016/j.ebiom.2022.103947.

23. Bouxsein ML, Boyd SK, Christiansen BA, Guldberg RE, Jepsen KJ, Müller R. Guidelines for assessment of bone microstructure in rodents using micro-computed tomography. *J Bone Miner Res*. 2010;**25**(7):1468–1486.

24. Zhang Y-g, Wu S, Lu R, et al. Tight junction CLDN2 gene is a direct target of the vitamin D receptor. *Sci Rep*. 2015;**5**:(1):10642.

25. Dror DK, Allen LH. Overview of nutrients in human milk. *Adv Nutr*. 2018;**9**(suppl_1):278S–294S.

26. Castro Dias M, Coisne C, Baden P, et al. Claudin-12 is not required for blood–brain barrier tight junction function. *Fluids Barriers CNS*. 2019;**16**(1):1–17.

27. Brenza HL, Kimmel-Jehan C, Jehan F, et al. Parathyroid hormone activation of the 25-hydroxyvitamin D3-1alpha-hydroxylase gene promoter. *Proc Natl Acad Sci USA*. 1998;**95**(4):1387–1391.

28. Christakos S, Li S, De L, Cruz J, et al. Vitamin D and the intestine: review and update. *J Steroid Biochem Mol Biol*. 2020;**196**:105501.

29. Mittermeier L, Demirkhanyan L, Stadlbauer B, et al. TRPM7 is the central gatekeeper of intestinal mineral absorption essential for postnatal survival. *Proc Natl Acad Sci USA*. 2019;**116**(10):4706–4715.

30. Cui M, Li Q, Johnson R, Fleet JC. Villin promoter-mediated transgenic expression of transient receptor potential cation channel, subfamily V, member 6 (TRPV6) increases intestinal calcium absorption in wild-type and vitamin D receptor knockout mice. *J Bone Miner Res*. 2012;**27**(10):2097–2107.

31. Cheung QC, Yuan Z, Dyce PW, Wu D, DeLange K, Li J. Generation of epidermal growth factor–expressing Lactococcus lactis and its enhancement on intestinal development and growth of early-weaned mice. *Am J Clin Nutr*. 2009;**89**(3):871–879.

32. Hu C, Xiao K, Luan Z, Song J. Early weaning increases intestinal permeability, alters expression of cytokine and tight junction proteins, and activates mitogen-activated protein kinases in pigs. *J Anim Sci*. 2013;**91**(3):1094–1101.

33. Stoutjesdijk E, Schaafsma A, Nhien NV, et al. Milk vitamin D in relation to the 'adequate intake' for 0–6-month-old infants: a study in lactating women with different cultural backgrounds, living at different latitudes. *Br J Nutr*. 2017;**118**(10):804–812.

34. Kraidith K, Jantarajit W, Teerapornpuntakit J, Nakkrasae L-i, Krishnamra N, Charoenphandhu N. Direct stimulation of the transcellular and paracellular calcium transport in the rat cecum by prolactin. *Pflugers Arch - Eur J Physiol*. 2009;**458**(5):993–1005.

35. Tanrattana C, Charoenphandhu N, Limlomwongse L, Krishnamra N. Prolactin directly stimulated the solvent drag-induced calcium transport in the duodenum of female rats. *Biochim Biophys Acta (BBA) - Biomembr*. 2004;**1665**(1–2):81–91.

36. Charoenphandhu N, Limlomwongse L, Krishnamra N. Prolactin directly stimulates transcellular active calcium transport in the duodenum of female rats. *Can J Physiol Pharmacol*. 2001;**79**(5):430–438.

37. Vass RA, Kiss G, Bell EF, et al. Breast milk for term and preterm infants-own mother's milk or donor milk? *Nutrients*. 2021;**13**(2):424.

38. Ikari A, Sato T, Watanabe R, Yamazaki Y, Sugatani J. Increase in claudin-2 expression by an EGFR/MEK/ERK/c-Fos pathway in lung adenocarcinoma A549 cells. *Biochim Biophys Acta (BBA) - Mol Cell Res*. 2012;**1823**(6):1110–1118.

39. Venugopal S, Anwer S, Szászi K. Claudin-2: roles beyond Permeability Functions. *IJMS*. 2019;**20**(22):5655.

40. Moran JR, Courtney ME, Orth DN, et al. Epidermal growth factor in human milk: daily production and diurnal variation during early lactation in mothers delivering at term and at premature gestation. *J Pediatr*. 1983;**103**(3):402–405.

41. Dvorak B, Fituch CC, Williams CS, Hurst NM, Schanler RJ. Increased epidermal growth factor levels in human milk of mothers with extremely premature infants. *Pediatr Res*. 2003;**54**(1):15–19.

42. Commare CE, Tappenden KA. Development of the infant intestine: implications for nutrition support. *Nutr Clin Pract*. 2007;**22**(2):159–173.

43. Alexander RT, Rievaj J, Dimke H. Paracellular calcium transport across renal and intestinal epithelia. *Biochem Cell Biol*. 2014;**92**(6):467–480.

44. Karbach U. Paracellular calcium transport across the small intestine. *J Nutr*. 1992;**122**(suppl_3):672–677.

45. Amnattanakul S, Charoenphandhu N, Limlomwongse L, Krishnamra N. Endogenous prolactin modulated the calcium absorption in the jejunum of suckling rats. *Can J Physiol Pharmacol*. 2005;**83**(7):595–604.

46. Karbach U. Segmental heterogeneity of cellular and paracellular calcium transport across the rat duodenum and jejunum. *Gastroenterology*. 1991;**100**(1):47–58.

47. Bronner F. Recent developments in intestinal calcium absorption. *Nutr Rev*. 2009;**67**(2):109–113.

48. Muniz LC, Menezes AMB, Buffarini R, Wehrmeister FC, Assunção MCF. Effect of breastfeeding on bone mass from childhood to adulthood: a systematic review of the literature. *Int Breastfeed J*. 2015;**10**(1):31.

49. Piyabhan P, Krishnamra N, Limlomwongse L. Changes in the regulation of calcium metabolism and bone calcium content during growth in the absence of endogenous prolactin and during hyperprolactinemia: a longitudinal study in male and female Wistar rats. *Can J Physiol Pharmacol*. 2000;**78**(10):757–765.

50. Matkovic V. Calcium metabolism and calcium requirements during skeletal modeling and consolidation of bone mass. *Am J Clin Nutr*. 1991;**54**(1):245S–260S.

51. Ghishan FK, Parker P, Nichols S, Hoyumpa A. Kinetics of intestinal calcium transport during maturation in rats. *Pediatr Res*. 1984;**18**(3):235–239.

52. Carpenter G. Epidermal growth factor is a major growth-promoting agent in human milk. *Science*. 1980;**210**(4466):198–199.

53. Dvorak B. Milk Epidermal Growth Factor and Gut Protection. *J Pediatr* 2010;**156**(2):S31–S35.

54. Gómez-Rial J, Curras-Tuala MJ, Talavero-González C, et al. Salivary epidermal growth factor correlates with hospitalization length in rotavirus infection. *BMC Infect Dis*. 2017;**17**(1):370.

55. Dagogo-Jack S. Epidermal growth factor EGF in human saliva: effect of age, sex, race, pregnancy and sialogogue. *Scand J Gastroenterol*. 1986;**21**:(sup124):47–54.

56. Hirai C, Ichiba H, Saito M, Shintaku H, Yamano T, Kusuda S. Trophic effect of multiple growth factors in amniotic fluid or human milk on cultured human fetal small intestinal cells. *J Pediatr Gastroenterol Nutr*. 2002;**34**(5):524–528.

57. Rowland KJ, Choi PM, Warner BW. The role of growth factors in intestinal regeneration and repair in necrotizing enterocolitis. *Semin Pediatr Surg*. 2013;**22**(2):101–111.

58. Kim TI, Poulin EJ, Blask E, et al. Myofibroblast keratinocyte growth factor reduces tight junctional integrity and increases claudin-2 levels in polarized Caco-2 cells. *Growth Factors*. 2012;**30**(5):320–332.

59. Stoutjesdijk E, Schaafsma A, Nhien NV, et al. Milk vitamin D in relation to the 'adequate intake' for 0-6-month-old infants: a study in lactating women with different cultural backgrounds, living at different latitudes. *Br J Nutr*. 2017;**118**(10):804–812.

60. Tsugawa N, Nishino M, Kuwabara A, et al. Comparison of vitamin D and 25-Hydroxyvitamin D concentrations in human breast milk between 1989 and 2016–2017. *Nutrients*. 2021;**13**(2):573.

61. Lou YR, Molnár F, Peräkylä M, et al. 25-Hydroxyvitamin D(3) is an agonistic vitamin D receptor ligand. *J Steroid Biochem Mol Biol*. 2010;**118**(3):162–170.

62. Mano H, Ikushiro S, Saito N, Kittaka A, Sakaki T. Development of a highly sensitive in vitro system to detect and discriminate between vitamin D receptor agonists and antagonists based on split-luciferase technique. *J Steroid Biochem Mol Biol*. 2018;**178**:55–59.

63. Verone-Boyle AR, Shoemaker S, Attwood K, et al. Diet-derived 25-hydroxyvitamin D3 activates vitamin D receptor target gene expression and suppresses EGFR mutant non-small cell lung cancer growth in vitro and in vivo. *Oncotarget*. 2016;**7**(1):995–1013.

64. Jiang H, Horst RL, Koszewski NJ, Goff JP, Christakos S, Fleet JC. Targeting 1,25(OH)2D-mediated calcium absorption machinery in proximal colon with calcitriol glycosides and glucuronides. *J Steroid Biochem Mol Biol*. 2020;**198**:105574.

65. Beggs MR, Bhullar H, Dimke H, Alexander RT. The contribution of regulated colonic calcium absorption to the maintenance of calcium homeostasis. *J Steroid Biochem Mol Biol*. 2022;**220**:106098. doi:10.1016/j.jsbmb.2022.106098.